18th International Conference on Information Fusion
Washington, DC - July 6-9, 2015

Joint estimation of target state and ionosphere state for OTHR based tracking

Hang Geng, Yan Liang, Feng Yang, Linfeng Xu
School of Automation, Northwestern Polytechnical University
Key laboratory of Information Fusion Technology, Ministry of Education
Xi'an, Shaanxi, 710072, P. R. China

***Abstract*—In over-the-horizon radars (OTHRs), the target state updates at a fast rate while the ionosphere state (e.g. the ionospheric height) evolves intermittently and all OTHR based tracking methods have the same prerequisite that the virtual ionospheric height, as the key model parameter in estimating the target state, should be obtained either by ionosondes or external sources. However, ionosondes can not be deployed arbitrarily and external sources may not be always available, resulting in the situation that the ionosphere state is unknown. It motivates us to consider the novel problem of multi-path target tracking in clutters without the help of ionosondes and external sources. The considered problem is formulated as the multi-rate state estimation with random coefficient matrices. First, the multi-rate state filter (MSF) with causality constraints is established for the multi-rate linear model. For the non-linear measurement model of OTHR, the derived MSF is extended to an iterative multi-rate state filter (IMSF) via the iterative optimization of joint state estimation and parameter identification (the linearized measurement matrix). In a numerical simulation about tracking two targets in four resolvable propagation modes our IMSF is testified.**

I. INTRODUCTION

The over-the-Horizon radar (OTHR) uses the refractive nature of high-frequency (HF) ionospheric propagation to perform wide-area surveillance of targets at long ranges beyond the horizon of conventional line-of-sight radars [1]-[3]. Different from traditional radars, OTHR faces the challenge of multi-path propagation, since it is often impossible to select a radar operating frequency that results in a single-mode propagation to the region of interest, so that multi-path propagation is unavoidable. By the fact that multiple radio-wave propagation paths or ray modes can result in multiple resolvable echoes from the same target [4], there exists the situation that more than one detection from the same target are obtained during a dwell or scan [5] [6]. In the presence of multiple ionospheric layers, multiple propagation paths between the transmitter/target and target/receiver give rise to multiple detections from a single target in the slant coordinates of the radar receiver. Much attention has been paid to the multi-path data association and fusion of OTHR which can be divided to the following two categories.

In the first category, state estimation based on Kalman filters and data association are implemented in the same coordinate (the slant or radar coordinate) in the process of which track fusion based on coordinate registration are involved, i.e., the mapping between slant coordinates and ground coordinates [7] [8]. In the second category, state estimate and data association are implemented in slant coordinates and ground coordinates, respectively, and hence twice mapping between slant coordinates and ground coordinates are needed. Its classical methods include multi-path data association (MPDA) [9]-[11], probabilistic multiple hypothesis tracking (PMHT) [12] [13] and multi-path Viterbi data association [14] [15]. Recently, there have been some developments on OTHR multitarget tracking such as multiple detection MHT (MD-MHT) [16], multiple detection JPDA (MD-JPDA)[17] and joint multipath data association and state estimation (JMAE) [18]. In general, these methods have the same requisite that the virtual ionospheric heights (the key parameter in coordinate registration) are given, for example by vertical and oblique ionosondes [19] [20]. As important components of OTHR systems, vertical and oblique ionosondes are utilized to detect the required virtual ionospheric height which might be unavailable due to the deployment constraints, for example, in the sea area or the hostile zone.

Recently, much attention has been paid to estimating the virtual ionospheric height by external sources such as beacons or transponders [8] [21] [22], terrain features [22], and forward-based receivers (FBRs) [23] [24]. However, the beacon-assisted method and the FBRs based method are only in effect within the limited zone, and the terrain-assisted method corrects the ground coordinates of each raymode roughly due to the large size of the resolution cell.

It is highly demanded to develop the novel target-tracking scheme for joint estimation of target state and ionosphere state without the help of ionosondes or external sources.

This paper presents the joint estimation problem of the fast-updating target state and intermittent-updating ionosphere state. The target state updates at a fast rate, while the ionospheric state evolves in a intermittent rate, i.e., changes abruptly and then remains constant for a period. Meanwhile, due to uncertainties of association relationship among measurements, tracks and possible propagation paths, the measurement model contains random coefficient matrices (RCM). First, the multi-rate linear system is lifted to an equivalent single-rate model with causality constraint, and the MSF is derived in the linear minimum mean square error (LMMSE) sense. Then the IMSF is developed via the iterative optimization of joint state estimation and parameter identification (the linearized measurement matrix) for the non-linear measure-

978-0-9964527-1-7©2015 ISIF

ment model case.

This article is organized as follows. The joint estimation problem of fast-updating multi-target states and intermittent-updating ionosphere state is formulated in Section 2. The original target tracking problem is reformulated as a multi-rate estimation problem with RCM, and the MSF and IMSE are designed in Section 3. A simulation testification is given in Section 4 and some conclusions are drawn in Section 5.

Throughout the paper, the superscripts "-1" and "T" represent the matrix inverse and transpose, respectively; the symbols "I " and "0 " represent identity and zero matrices with proper dimensions, respectively; diag$\{\cdot\}$ denotes a block diagonal matrix; $E\{\cdot\}$ is the mathematical expectation; E^* is the LMMSE estimation operator; trace$\{\cdot\}$ is the matrix trace; $(\cdot)$ denotes the same contents as that in the previous parenthesis.

II. Problem Formulation

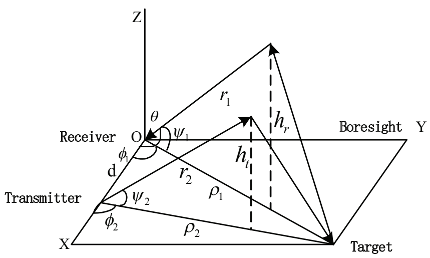

Fig. 1. Geometry of planar OTHR measurement model

Fig. 1 depicts the geometry of the target and radar sensor system of bistatic OTHR. The ray paths from the transmitter/target to the target/receiver are assumed to be reflected from the ionosphere at virtual height h_t/h_r. The electronic concentration of the ionosphere changes tardily and then stays invariable within some periods results in the intermittent evolvement of the equivalent heights of the reflecting ionosphere. In OTHR based target tracking, the target state updates at a fast rate while the ionosphere state (e.g. the ionospheric height) evolves intermittently. In other words, there exists a multi-rate system model of fast-updating target states and intermittent-updating ionosphere states [9]. Traditionally, the ionospheric height is obtained by vertical and oblique ionosondes or external sources of information from beacons, transponders, terrain features, FBRs, etc. However, because of the limited deployment of ionosondes, and external sources of information may be corrupted by environmental or enemy disturbances, the virtual ionospheric height is not always known accurately. It motivates us to develop the joint estimation scheme of target state and ionosphere state.

A. Multi-target and ionospheric dynamic model

Consider the following multi-rate system.

- the fast-updating dynamic subsystem P_1 of tracking t targets:

$$x_{1m,k+1} = A_{1m}x_{1m,k} + B_{1m}u_{1m,k} + \Gamma_{1m}\omega_{1m,k}, \quad m = 1,\cdots,t, \tag{1}$$

or its compact equivalent form

$$X_{1,k+1} = A_1X_{1,k} + B_1u_{1,k} + \Gamma_1\omega_{1,k}, \tag{2}$$

with

$$\begin{aligned} X_{1,k} &= \text{col}\{x_{11,k},\cdots,x_{1t,k}\}, \\ A_1 &= \text{diag}\{A_{11},\cdots,A_{1t}\}, \\ B_1 &= \text{diag}\{B_{11},\cdots,B_{1t}\}, \\ \Gamma_1 &= \text{diag}\{\Gamma_{11},\cdots,\Gamma_{1t}\}, \\ u_{1,k} &= \text{col}\{u_{11,k},\cdots,u_{1t,k}\}, \\ \omega_{1,k} &= \text{col}\{\omega_{11,k},\cdots,\omega_{1t,k}\}, \end{aligned}$$

- the intermittent-evolving subsystem, i.e., the slow-updating system P_2 plus a holder H:

$$P_2 : x_{2,kN+N} = A_2x_{2,kN} + B_2u_{2,kN} + \Gamma_2\omega_{2,kN}, \tag{3}$$

$$H : x_{2,kN+i} = x_{2,kN}, i = 1,2,\ldots,N-1, \tag{4}$$

where $x_{1m,k} \in \Re^{n_1}$ is the fast-updating target state evolving at a basic period h;
$x_{1m,k} = \text{col}\{\rho_{1m,k},\ \dot{\rho}_{1m,k},\ b_{1m,k},\ \dot{b}_{1m,k}\}$ represent the ground range, range rate, azimuth and azimuth rate, respectively; $x_{2,k} \in \Re^{n_2}$ is the state of ionospheric height updating at the period kNh and remains constant in the next $(N-1)h$ period, and $x_{2,k} = \text{col}\{h_i,\ i = 1,\cdots,\gamma\}$, where γ is the number of ionosphere layers. $u_{1m,k} \in \Re^r$ and $u_{2,k} \in \Re^n$ are known inputs; $\omega_{1m,k}$ and $\omega_{2,k}$ are zero-mean white noises with known covariances $Q_{1m,k}$ and $Q_{2,k}$, respectively; matrices A_{1m}, B_{1m}, Γ_{1m}, A_2, B_2 and Γ_2 are known with proper dimensions. Here $\omega_{1m,k}$ and $\omega_{2,k}$ are mutually and independent of each other.

B. OTHR measurement model for multi-path propagation

The radar measurements consist of the slant range $Rg = r_1 + r_2$ (half of the path length), Doppler Rr (the rate of the change of the slant range), and azimuth $Az = \pi/2 - \theta$. Each scan of the OTHR consists of a set of m_k measurements:

$$z_{k,j} = \text{col}\{Rg_{k,j}, Rr_{k,j}, Az_{k,j}\},\ j = 1,2,\cdots,m_k. \tag{5}$$

The measurement of OTHR may originate from the interested target via one possible propagation path or just clutter. If $z_{k,j}$ comes from the interested target with the l_2-th forward propagation and the l_1-th backward propagation, then the measurement model with respect to target states and ionospheric heights are

$$z_{k,j} = \begin{cases} H^{m,s}_{k,j}(x_{1m,k}, x_{2,k}) + v_{k,j}, & \theta_{k,j} = m^s, \\ \Theta_{k,j}, & \theta_{k,j} = 0, \end{cases} \tag{6}$$

where $v_{k,j} \in R^{n_z}$ is zero-mean and white with the known covariance $R_{k,j}$; $\theta_{k,j} = m^s$ represents the measurement $z_{k,j}$ is received from target m via mode s; $s = L_{l_1,l_2}, l_1 = 1,\cdots,L_1, l_2 = 1,\cdots,L_2$ represents the (l_1,l_2)-th propagation mode, L_1 and L_2 are the numbers of the possible virtual ionospheric reflecting layer for backward and forward paths, respectively. $\theta_{k,j} = 0$ represents the measurement $z_{k,j}$ is independent clutter $\Theta_{k,j}$. The nonlinear target-oriented measurement $H_{k,j}^{m,s}$ is given by

$$H_{k,j}^{m,s} = \begin{pmatrix} r_{1,k}^{l_1} + r_{2,k}^{l_2} \\ (\rho_{1m,k}/r_{1,k}^{l_1} + \eta_{1m,k}/r_{2,k}^{l_2})\dot{\rho}_{1m,k}/4 \\ sin^{-1}\{\rho_{1m,k} sin(b_{1m,k})/(2r_{1,k}^{l_1})\} \end{pmatrix}, \quad (7)$$

with

$$\begin{aligned} r_{1,k}^{l_1} &= \sqrt{(\rho_{1m,k}/2)^2 + (h_k^{r,l_1})^2}, \\ r_{2,k}^{l_2} &= \sqrt{\frac{\rho_{1m,k}^2}{4} - \frac{d\rho_{1m,k} sin(b_{1m,k})^2}{4}\frac{d^2}{4} + (h_k^{t,l_2})^2}, \\ \eta_{1m,k} &= \rho_{1m,k} - dsin(b_{1m,k}), \end{aligned}$$

where h_k^{t,l_2} and h_k^{r,l_1} are the unknown virtual heights respectively, representing the heights of the reflection points in forward path (from the transmitter to the target) and backward path (from the target to the receiver) related to $z_{k,j}$.

As mentioned in [9] each propagation mode $s, s \in (l_1, l_2)$ produces an echo with certain probability of detection. For simplicity, these probability are considered identical and denoted by $P_D (P_D \le 1)$.

The clutter (false measurement) model is specified by a 3-dimensional probability density function (PDF) $p_c(y_k)$. Clutter detections are assumed to be independent from scan to scan. The most commonly-used clutter spatial distribution is uniform clutter as follows.

$$p_c(\Theta_k) = \begin{cases} V^{-1}(k), \ \Theta_k \in G(k), \\ 0, \qquad \text{otherwise}, \end{cases} \quad (8)$$

and the clutter number obeys the Possion distribution, i.e., the probability function $g_c(n)$ for the number of clutter measurements n within the validation region is given:

$$g_k^c(\delta) = \text{Probability}\{g_k^c = \delta\} = \frac{(\lambda V(k))^\delta e^{-\lambda V(k)}}{\delta!}, \quad (9)$$

where $\delta = 0, 1, 2, \cdots$; λ is taken as N_k/V_s, and N_k is the total number of clutters in the scan; V_s is the volume of the corresponding space and $G(k)$ is the interested zone.

Traditionally, the ionospheric heights are provided by ionosondes or external sources of information, and hence the target tracking problem of OTHR can be solved through the combination of data association and nonlinear filters . Here we derive the joint estimation of target states and ionospheric states without the help of ionosondes and external sources of information.

III. Filter Design

In this section, we will derive a multi-rate joint state filter. In the first place, we design the multi-rate LMMSE filter for a linear state and measurement model, and then extend the result to the nonlinear case through iterative optimization.

A. MSF design for linear measurement model

Consider the measurement in (6) with the following linear expression.

$$\begin{aligned} z_{k,j} &= H_{k,j}^{m,s}(x_{1m,k}, x_{2,k}) + v_{k,j} \\ &= C_{1,k,j}^{m,s} x_{1m,k} + C_{2,k,j}^{m,s} x_{2,k} + v_{k,j}, \\ & j = 1, 2, \cdots, m_k, \end{aligned} \quad (10)$$

Suppose that there are s propagation modes at time instant k, and the measurement $z_{k,j}$ is received from target $m, m \in (1, \ 2, \cdots, \ t)$ via mode $s \in (l_1, l_2)$, $l_1 = 1, \cdots, L_1, l_2 = 1, \cdots, L_2$, with probability $p_{k,j}^{m,s}$ which can be calculated by the same method used in the event association part of MPDA [9] or JPDA [25]. Then, for any a measurement $z_{k,j}$, the corresponding measurement coefficient matrix

$$\begin{aligned} &\begin{bmatrix} C_{1,k,j} & C_{2,k,j} \end{bmatrix} \\ = &\begin{cases} \begin{bmatrix} C_{1,k,j}^{1,L_{1,1}} & 0\cdots & C_{2,k,j}^{1,L_{1,1}} \end{bmatrix}, \text{prob } p_{k,j}^{1,L_{1,1}}, \\ \quad \vdots \quad \vdots \quad \vdots \quad \vdots \\ \begin{bmatrix} C_{1,k,j}^{t,L_{L_2,L_1}} & 0\cdots & C_{2,k,j}^{t,L_{L_2,L_1}} \end{bmatrix}, \text{prob } p_{k,j}^{t,L_{L_2,L_1}}. \end{cases} \end{aligned} \quad (11)$$

where $prob$ stands for probability. (10) is rewritten as

$$z_{k,j} = \overline{C}_{1,k,j} X_{1,k} + \overline{C}_{2,k,j} x_{2,k} + \tilde{v}_{k,j}, \quad (12)$$

with

$$\begin{aligned} \overline{C}_{1,k,j} &= E\{C_{1,k,j}\}, \ \overline{C}_{2,k,j} = E\{C_{2,k,j}\}, \\ \tilde{C}_{1,k,j} &= C_{1,k,j} - \overline{C}_{1,k,j}, \ \tilde{C}_{2,k,j} = C_{2,k,j} - \overline{C}_{2,k,j}, \\ \tilde{v}_{k,j} &= \tilde{C}_{1,k,j} X_{1,k} + \tilde{C}_{2,k,j} x_{2,k} + v_{k,j}. \end{aligned}$$

For the convenience of obtaining the optimal parameter for the multi-rate state filter (MSF), we transform the original multi-rate time-varying system into an equivalent single-rate system. Through lifting technique [26], the above multi-rate state estimation with random coefficient matrices is reformulated as the following single-rate lifted system

$$\begin{aligned} \underline{x}_k &= \underline{A} \ \underline{x}_{k-1} + \underline{B} \ \underline{u}_{k-1} + \underline{\Gamma} \ \underline{\omega}_{k-1}, && (13) \\ \underline{z}_k &= \underline{C}_k \ \underline{x}_k + \underline{v}_k, && (14) \end{aligned}$$

with

$$\begin{aligned} \underline{x}_k &= \text{col}\{X_{1,kN}, \cdots, X_{1,kN+N-1}, x_{2,kN}\}, \\ \underline{z}_k &= \text{col}\{z_{kN,1}, \cdots, z_{kN,m_{kN}}, \\ &\quad \cdots, z_{kN+N-1,1}, \cdots, z_{kN+N-1,m_{kN+N-1}}\}, \\ \underline{v}_k &= \text{col}\{\tilde{v}_{kN,1}, \cdots, \tilde{v}_{kN,m_{kN}}, \\ &\quad \cdots, \tilde{v}_{kN+N-1,1}, \cdots, \tilde{v}_{kN+N-1,m_{kN+N-1}}\}, \\ \underline{u}_{k-1} &= \text{col}\{u_{1,kN-1}, \cdots, u_{1,kN+N-2}, u_{2,kN-N}\}, \\ \underline{w}_{k-1} &= \text{col}\{w_{1,kN-1}, \cdots, w_{1,kN+N-2}, w_{2,kN-N}\}, \\ \underline{A} &= \begin{bmatrix} 0 & \ldots & 0 & A_1 & 0 \\ 0 & \ldots & 0 & A_1^2 & 0 \\ \vdots & & \ldots & \vdots & \vdots \\ 0 & \ldots & 0 & A_1^N & 0 \\ 0 & \ldots & \ldots & 0 & A_2 \end{bmatrix}, \end{aligned}$$

$$\underline{B} = \begin{bmatrix} B_1 & & & & \\ A_1B_1 & B_1 & & & \\ \vdots & \ddots & \ddots & & \\ A_1^{N-1}B_1 & A_1^{N-2}B_1 & \cdots & B_1 & \\ 0 & 0 & \cdots & 0 & B_2 \end{bmatrix},$$

$$\underline{\Gamma} = \begin{bmatrix} \Gamma_1 & & & & \\ A_1\Gamma_1 & \Gamma_1 & & & \\ \vdots & \ddots & \ddots & & \\ A_1^{N-1}\Gamma_1 & A_1^{N-2}\Gamma_1 & \cdots & \Gamma_1 & \\ 0 & 0 & \cdots & 0 & \Gamma_2 \end{bmatrix},$$

$$\underline{C}_k = \begin{bmatrix} \overline{C}_{1,kN} & 0 & 0 & \overline{C}_{2,kN} \\ 0 & \overline{C}_{1,kN+1} & & \overline{C}_{2,kN+1} \\ \vdots & \ddots & \ddots & \vdots \\ 0 & 0 & \overline{C}_{1,kN+N-1} & \overline{C}_{2,kN+N-1} \end{bmatrix},$$

$$\begin{aligned} \overline{C}_{1,kN+i} &= \mathrm{col}\{\overline{C}_{1,kN+i,m_1},\cdots,\overline{C}_{1,kN+i,m_{kN+i}}\}, \\ & \quad i=0,1,\cdots, \\ \overline{C}_{2,kN+i} &= \mathrm{col}\{\overline{C}_{2,kN+i,m_1},\cdots,\overline{C}_{2,kN+i,m_{kN+i}}\}, \end{aligned}$$

where $\underline{\omega}_{k-1}$ is zero-mean and white with covariance $\underline{Q}_{k-1} = \mathrm{diag}\{Q_{1,kN-1},\cdots,Q_{1,kN+N-2},Q_{2,kN-N}\}$; $\underline{v}_k$ is dependent of two periodical-varying states.

The recursive calculation of $R_{\tilde{v}_{k,j}}$ is derived as follows. Denote $\Pi_k = E(X_{1,k}X_{1,k}^T)$, $\varepsilon_k = E(x_{2,k}x_{2,k}^T)$, $d_{a,b} = E\left[(\tilde{C}_{1,k,j})_{a,b}(\tilde{C}_{1,k,j})_{b,a}\right]$, $e_{a,b} = E\left[(\tilde{C}_{2,k,j})_{a,b}(\tilde{C}_{2,k,j})_{b,a}\right]$, and define F as a matrix with its (a,b)-th element being 1 and others being 0. By the fact that $\tilde{v}_{k,j}$ is independent of states, the recursive calculation of $R_{\tilde{v}_{k,j}}$ is given by

$$\begin{aligned} R_{\tilde{v}_{k,j}} &= R_{v_{k,j}} + \\ & \quad \sum_{a,b}\left[(\Pi_{k+1})_{a,b}d_{a,b}F_{a,b} + (\varepsilon_{k+1})_{a,b}e_{a,b}F_{a,b}\right], \end{aligned} \tag{15}$$

with

$$\Pi_{k+1} = A_1\Pi_kA_1^T + B_1u_{1,k}u_{1,k}^TA_1^T + \Gamma_1Q_{1,k}\Gamma_1^T, \tag{16}$$

$$\varepsilon_{k+1} = A_2\varepsilon_kA_2^T + B_2u_{2,k}u_{2,k}^TA_2^T + \Gamma_2Q_{2,k}\Gamma_2^T. \tag{17}$$

Denote $\hat{x}_{i,j|k} = E^*[x_{i,j}|Z^k]$, and the state estimation, state prediction, covariance estimation and covariance prediction for the lifted system by (13)-(14) can be represented as

$$\begin{aligned} \underline{\hat{x}}_k^e &= \mathrm{col}\{\hat{x}_{11,kN|kN},\cdots,\hat{x}_{11,kN+N-1|kN+N-1}, \\ & \quad \cdots,\hat{x}_{1t,kN|kN},\cdots,\hat{x}_{1t,kN+N-1|kN+N-1},\hat{x}_{2,kN|kN}\}, \\ \underline{\hat{x}}_k^p &= \mathrm{col}\{\hat{x}_{11,kN|kN-1},\cdots,\hat{x}_{11,kN+N-1|kN-1}, \\ & \quad \cdots,\hat{x}_{1t,kN|kN-1}\hat{x}_{1t,kN+N-1|kN-1},\hat{x}_{2,kN|kN-1}\}, \\ \underline{P}_k^e &= E\{(\underline{x}_k^e - \underline{\hat{x}}_k^e)(\cdot)^T\},\ \underline{P}_k^p = E\{(\underline{x}_k^p - \underline{\hat{x}}_k^p)(\cdot)^T\}. \end{aligned}$$

Remark 1: The direct utilization of the standard Kalman filter on the lifted system in (13)-(14) would result in the interval smoother of the original multi-rate system instead of the desirable filter by the fact that the measurements at different times are lifted as one equivalent measurement. In other words, the filter for the lifted system with causality constraint should be studied

Theorem 1: For the multi-rate model in (1)-(4) with its corresponding linear measurement in (12), its LMMSE filter has the following recursion

$$\begin{aligned} \hat{x}_{1m,kN+i|kN-1} &= A_{1m}^i\hat{x}_{1m,(k-1)N+i|(k-1)N+i-1} \\ & \quad + \sum_{j=1}^{N-1}A_{1m}^{N-j}B_{1m}u_{kN+j-2}, \\ & \quad i=0,\cdots,N-1, \end{aligned} \tag{18}$$

$$\begin{aligned} \hat{x}_{1m,kN+i|kN+i} &= \hat{x}_{1m,kN+i|kN-1} + \sum_{j=1}^{i+1}\underline{K}^{i,j} \\ & \quad (\bar{z}_{kN+i} - \bar{C}_{1,kN+i}\hat{x}_{1m,kN+i|kN-1} \\ & \quad -\bar{C}_{2,kN+i}\hat{x}_{2,kN|kN-1}), \end{aligned} \tag{19}$$

$$\begin{aligned} \hat{x}_{2,kN|kN} &= \hat{x}_{2,kN|kN-1} + \sum_{j=1}^{N}\underline{K}^{N+1,j} \\ & \quad (\bar{z}_{kN+N-1} - \\ & \quad \bar{C}_{1,kN+N-1}\hat{x}_{1,kN+N-1|kN-1} \\ & \quad -\bar{C}_{2,kN+N-1}\hat{x}_{2,kN|kN-1}), \end{aligned} \tag{20}$$

$$\begin{aligned} \hat{x}_{2,kN+i|kN-1} &= \hat{x}_{2,kN|kN-1} + \sum_{j=1}^{i+1}\underline{K}^{N+1,j} \\ & \quad (\bar{z}_{kN+i} - \bar{C}_{1,kN+i}\hat{x}_{1,kN+i|kN-1} \\ & \quad -\bar{C}_{2,kN+i}\hat{x}_{2,kN|kN-1}), \end{aligned} \tag{21}$$

$$\begin{aligned} \hat{z}_{kN+i|kN-1,m_{kN+i}} &= C_{1,kN+i,m_{kN+i}}\hat{x}_{1m,kN+i|kN-1} + \\ & \quad C_{2,kN+i,m_{kN+i}}\hat{x}_{2,kN+i|kN-1}, \end{aligned} \tag{22}$$

$$\begin{aligned} \underline{P}_k^{p(i,j)} &= \sum_{l=1}^{N+1}\sum_{q=1}^{N+1}\underline{A}^{(i,l)}\underline{P}_{k-1}^{e(i,j)}\underline{A}^{(j,q)} \\ & \quad + \sum_{l=1}^{N+1}\sum_{q=1}^{N+1}\underline{\Gamma}^{(i,l)}\underline{Q}_{k-1}^{(i,j)}\underline{\Gamma}^{(j,q)}, \\ & \quad i,j=1,\cdots,N+1, \end{aligned} \tag{23}$$

$$\begin{aligned} \underline{P}_k^{e(i,j)} &= \sum_{l=1}^{N+1}\sum_{q=1}^{N+1}(I - \sum_{s=1}^{i}\underline{K}_k^{i,s}\underline{C}_k^{(s,l)})\underline{P}_k^{p(l,q)} \\ & \quad (I - \sum_{n=1}^{i}\underline{C}_k^{(j,n)}\underline{K}_k^{n,q}) + \sum_{r=1}^{N+1}\sum_{p=1}^{N+1}\underline{K}_k^{i,r}\underline{R}_k^{(r,p)}\underline{K}_k^{j,p}, \end{aligned} \tag{24}$$

$$\underline{K}_k = \begin{bmatrix} \underline{K}_k^{1,1} & & & \\ \vdots & \ddots & \ddots & \\ \underline{K}_k^{N,1} & \underline{K}_k^{N,2} & \cdots & \underline{K}_k^{N,N} \\ \underline{K}_k^{N+1,1} & \underline{K}_k^{N+1,2} & \cdots & \underline{K}_k^{N+1,N} \end{bmatrix}, \tag{25}$$

with

$$\bar{z}_{kN} = \mathrm{col}\{z_{kN,1},\cdots,z_{kN,m_{kN}}\},$$

$$
\begin{aligned}
K_k^i &= \begin{cases} \left[\underline{K}_k^{(i,1)}, \underline{K}_k^{(i,2)}, \cdots, \underline{K}_k^{(i,i)}\right], i = 1, 2, \cdots, N-1, \\ \left[\underline{K}_k^{(i,1)}, \underline{K}_k^{(i,2)}, \cdots, \underline{K}_k^{(i,N)}\right], i = N, N+1, \end{cases} \\
&= U_k^(i)(V_k^(i))^{-1}, \\
U_k^{(i)} &= \begin{cases} \begin{bmatrix} \underline{P}_k^{p(i,1)} & \underline{P}_k^{p(i,2)} & \cdots & \underline{P}_k^{p(i,i)} \end{bmatrix} \bar{C}_{1,r}^T \\ +1_i^T \otimes \underline{P}_k^{p(i,N+1)} \bar{C}_{2,r}^T, \ i = 1, 2, \cdots, N-1, \\ \begin{bmatrix} \underline{P}_k^{p(i,1)} & \underline{P}_k^{p(i,2)} & \cdots & \underline{P}_k^{p(i,N)} \end{bmatrix} \bar{C}_{1,r}^T \\ +1_N^T \otimes \underline{P}_k^{p(i,N+1)} \bar{C}_{2,r}^T, \ i = N, N+1, \end{cases} \\
V_k^{(i)} &= \begin{cases} C_k^{(i)} \underline{P}_k^p \ (C_k^{(i)})^T + R_{\underline{v}_k}^{(i)}, i = 1, \cdots, N-1, \\ \underline{C}_k \ \underline{P}_k^p \ (\underline{C}_k)^T + R_{\underline{v}_k}^{(i)}, i = N, N+1, \end{cases} \\
R_{\underline{v}_k} &= \mathrm{diag}\{\tilde{v}_{kN,1}, \cdots, \tilde{v}_{kN,\beta_{kN}}, \cdots, \tilde{v}_{kN+N-1,1}, \\
& \quad \cdots, \tilde{v}_{kN+N-1,\beta_{kN+N-1}}\},
\end{aligned}
$$

where $\underline{P}_k^{p(i,j)}$ and $\underline{P}_k^{e(i,j)}$ are the (i,j)-th sub-block of $\underline{P}_k^p$ and $\underline{P}_k^e$, respectively; $\underline{A}^{(i,j)}$, $\underline{\Gamma}^{(i,j)}$, $\underline{C}_k^{(i,j)}$ and $\underline{R}_k^{(i,j)}$ are the (i,j)-th sub-block of the corresponding matrices, respectively; K_k^i, U_k^i, V_k^i and $R_{\underline{v}_k}^{(i)}$ are the i-th row of K_k, U_k, V_k and $R_{\underline{v}_k}$, respectively; $K_k^{(i,j)}$ is the (i,j)-th sub-block of K_k.

Proof: See the Appendix.

Remark 2: As shown in (25), there exist $N(N-1)/2$ zero-valued blocks in $\underline{K}_k$. This is due to the causality constraint, i.e., the future measurements can not be utilized in the current estimate in the filter design.

Remark 3: It's worth to mention that the proposed MSF in (18)-(25) is quite different from the standard Kalman filter. In our MSF, the state filtering $\hat{x}_{1m,kN+i|kN+i}$ is calculated from the $i+1$ step state prediction $\hat{x}_{1m,kN+i|kN-1}$, instead of $\hat{x}_{1m,kN+i|kN+i-1}$. In other words, though the state x_{1m} updates at the fast rate equaling to the sensor sampling rate, its estimate updates much different compared with the Kalman filter due to the effect of the intermittent-updating state $x_{2,k}$.

B. IMSF design for non-linear measurement model

For the non-linear measurement in (6), the choice of the linearized point determines the linearisation error, and further determines the estimation accuracy. Hence, the idea of obtaining more accurate state estimates motivates us to introduce the framework of iterative optimization (the idea of iteration in the filter design has been reported in many researches [27]-[30]).

Define the linearized point $x_k^{(l)} (l = 0, 1, \cdots, L, L \geq 1)$ by

$$
x_k^{(l)} = \begin{cases} col\{x_{1m,kN+i|kN-1}^{(l)}, x_{2,kN+i|kN-1}^{l}\}, l = 0, \\ col\{x_{1m,kN+i|kN+i}^{(l)}, x_{2,kN+i|kN+i}^{l}\}, l \in \{1, \cdots, L\}, \end{cases} \tag{26}
$$

where $l = 0, 1, \cdots, L$ denotes the current iteration number and L is the maximum iteration number; $x_k^{(l)}$ represents the state estimation in the l-th iteration. The recursive implementation of the IMSF is shown in Fig. 2. In Fig. 2, the linearisation matrix

$$
\begin{aligned}
&\begin{bmatrix} C_{1,kN+i,j}^{m,s(l)} & C_{2,kN+i,j}^{m,s(l)} \end{bmatrix} \\
&= \left. \frac{\partial H_{k,j}^{m,s}(x_{1m,k}, x_{2,k})}{\partial x_k} \right|_{x_k = col\{x_{1m,kN+i}^{(l)}, x_{2,kN+i}^{(l)}\}} . \quad (27)
\end{aligned}
$$

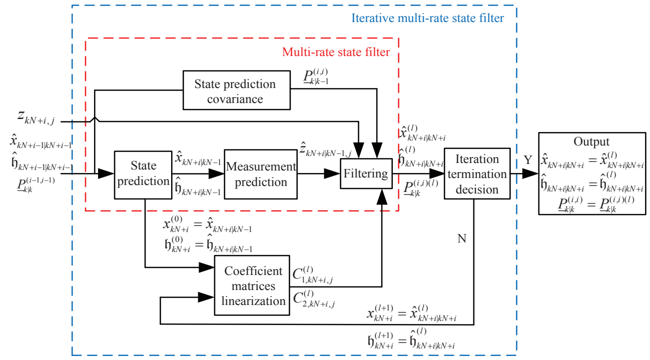

Fig. 2. Recursive implementation of the IMSF

is the equivalent measurement matrix, and hence the non-linear measurement model in (6) is transformed into the linear one in (12).

As shown in Fig. 2, the iteration and the filtering is interweaved, and the close loop feedback is introduced in the filtering process to obtain the better linearization points, resulting in the improvement of filtering accuracy.

Remark 4: The iteration strategy, which aims at eliminating the coupled errors and optimize the linearized points, is realized by letting the linearized point col$\{x_{1m,kN+i}^{(l)}, x_{2,kN+i}^{(l)}\}$, $(l \in \{0, 1, \cdots, L, L \geq 1\})$ equal to the latest state estimation col$\{\hat{x}_{1m,kN+i|kN+i}^{(l-1)}, \hat{x}_{2,kN+i|kN+i}^{(l-1)}\}$ in matrix $[C_{1,kN+i,j}^{m,s(l)} \quad C_{2,kN+i,j}^{m,s(l)}]$ and then the state is estimated repeatedly. Hence, the estimation precision can be improved greatly because $[C_{1,kN+i,j}^{m,s(l)} \quad C_{2,kN+i,j}^{m,s(l)}]$ is calculated iteratively. The iteration is stopped until the following iteration terminate condition (relative estimation error) is satisfied

$$
\frac{\parallel \hat{x}_k^{(l+1)} - \hat{x}_k^{(l)} \parallel_2}{\parallel \hat{x}_k^{(l)} \parallel_2} \leq \varepsilon \quad or \quad l > L(l \in \{1, \cdots, L\}), \tag{28}
$$

where $\varepsilon(0 < \varepsilon \leq 1)$ is the set iteration accuracy threshold. $\parallel A \parallel_2$ denotes the 2-norm of vector A. If (28) holds, the state estimate and its covariance will be determined by $col\{\hat{x}_{1m,kN+i|kN+i}, \hat{x}_{2,kN+i|kN+i}\} = col\{\hat{x}_{1m,kN+i|kN+i}^{(l)}, \hat{x}_{2,kN+i|kN+i}^{(l)}\}$ and $\underline{P}_k^{e(i,i)} = \underline{P}_k^{e(i,i)(l)}$, respectively.

In Fig. 2, the purpose of the coefficient matrix linearization block is to optimize matrix $[C_{1,kN+i,j}^{m,s(l)} \quad C_{2,kN+i,j}^{m,s(l)}]$ iteratively using linearized points col$\{x_{1m,kN+i}^{(l)}, x_{2,kN+i}^{(l)}\}$, $(l = 0, 1, \cdots, L, L \geq 1)$, which are obtained from the initial state prediction and the state estimation of every iteration process. The iteration termination decision block, acting as the feedback control block, is used to make a decision about whether the state estimation result feedbacks to the coefficient matrix linearization block to reconstruct the coefficient matrix. It is the basis of iterative optimization and is vital to the filter design.

Remark 5: As shown in Fig. 2 the proposed IMSF is a joint optimization method. The coefficient matrix linearization and the state estimation are unified in an iterative optimisation framework. The state estimation via the l-th iteration is utilized as the linearized points in determining $[C^{m,s(l)}_{1,kN+i,j} \quad C^{m,s(l)}_{2,kN+i,j}]$ for the $(l+1)$-th iteration, and such iteration brings out the close loop in data processing. In the views of feedback control, such resultant close loop is helpful in obtaining better accuracy.

The iteration procedure of the IMSF is given in Table 1.

TABLE I
CALCULATION STEPS OF THE IMSF SCHEME

Step 1.Prediction: Compute $\hat{x}_{1m,kN+i\|kN-1}$, $\hat{x}_{2,kN+i\|kN-1}$, $\hat{z}_{kN+i\|kN-1,n_{kN+i}}$, and $\underline{P}^{p(i,i)}_{k}$ by (18), (21)-(23), respectively.
Step 2. Coefficient matrix linearization: Determine the linearised point col$\{x^{(l)}_{1m,kN+i}, x^{(l)}_{2,kN+i}\}$, and calculate matrix $[C^{m,s(l)}_{1,kN+i,j} \quad C^{m,s(l)}_{2,kN+i,j}]$.
Step 3. Filter gain: Compute the filter gain $\underline{K}^{(i,i)}_{k}$ by (25).
Step 4. Estimation: Update the state estimation $\hat{x}^{(l)}_{1m,kN+i\|kN+i}$, $\hat{x}^{(l)}_{2,kN+i\|kN+i}$, and $\underline{P}^{e(i,i)(l)}_{k}$ by (19), (20), and (24), respectively.
Step 5. Iteration terminate decision: Compute the relative estimation error by (28). If (28) holds, go to Step 6.Else let col$\{x^{(l+1)}_{1m,kN+i}, x^{(l+1)}_{2,kN+i}\}$ =col$\{\hat{x}^{l}_{1m,kN+i\|kN+i}, \hat{x}^{l}_{2,kN+i\|kN+i}\}$, and go to Step 2 while $l = l+1$.
Step 6. Output: Output the state estimation $\hat{x}_{1m,kN+i\|kN+i} = \hat{x}^{l}_{1m,kN+i\|kN+i}$, $\hat{x}_{2,kN+i\|kN+i} = \hat{x}^{l}_{2,kN+i\|kN+i}$, and the covariance estimation $\underline{P}^{e(i,i)}_{k} = \underline{P}^{e(i,i)}_{k}$.

IV. SIMULATION RESULTS

The simulation considers a scenario of two non-maneuvering targets in the ground coordinates with an average false measurement density of 400 points per dwell [9]. The parameters in (1)-(4) are

$$
\begin{aligned}
A_{11} &= \begin{bmatrix} 1 & 1 \\ 0 & 1 \end{bmatrix} \otimes I_2, \Gamma_{11} = [0.5, 1]^T, B_{11} = O_{4\times 1}, \\
A_{12} &= \mathrm{diag}\{F_1, F_2\}, \Gamma_{12} = \Gamma_{11}, B_{12} = O_{4\times 1}, \\
F_1 &= \begin{bmatrix} \cos(2\pi/300) & \sin(2\pi/150) \\ -\sin(2\pi/300) & \cos(2\pi/150) \end{bmatrix}, \\
F_2 &= \begin{bmatrix} \cos(2\pi/150) & \sin(2\pi/300) \\ -\sin(2\pi/150) & \cos(2\pi/300) \end{bmatrix}, \\
Q_{11} &= Q_{12} = \mathrm{diag}\{7.830\times 10^{-6}, 1.303\times 10^{-6}, \\
&\quad 1.491\times 10^{-12}, 1.118\times 10^{-14}\}, \\
R &= \mathrm{diag}\{25, 10^{-6}, 9\times 10^{-6}\}.
\end{aligned}
$$

Independent multi-path propagation is assumed via EE, EF, FE and FF modes, with initial ionospheric heights set as $h_E = 100km$ and $h_F = 220km$. The probability of target detection for each propagation mode is 0.4. The gate probability is $P_G = 0.971$, i.e., the tracking gates size is $\gamma = 16$. The revisit period is $T = 10s$. The initial values

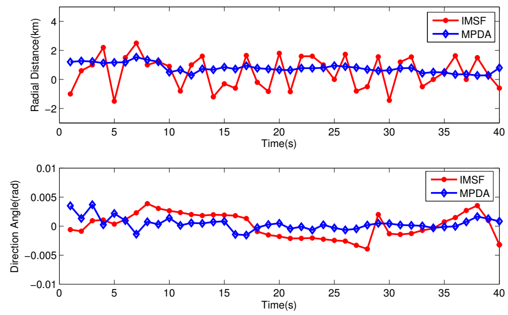

Fig. 3. Estimation error of target 1

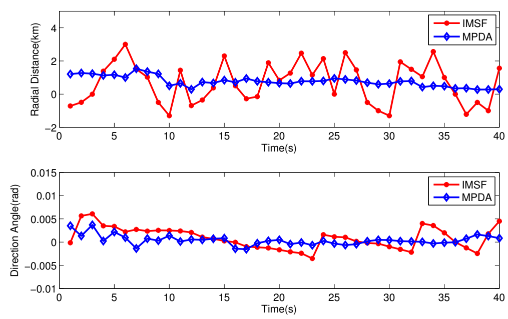

Fig. 4. Estimation error of target 2

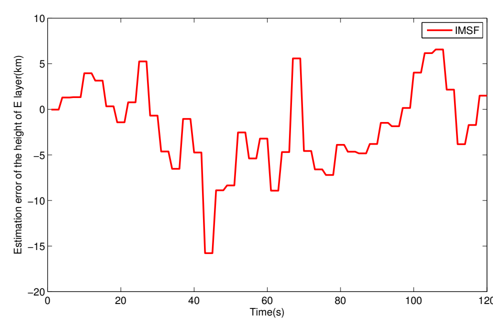

Fig. 5. Estimation error of ionosphere layer E

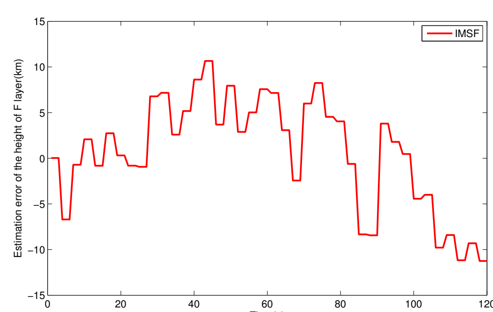

Fig. 6. Estimation error of ionosphere layer F

of target state and error covariance are

$$\begin{aligned}
x_{11}(0) &= [1100, 0.15, 1.46528, 8.72\times10^{-5}]^T,\\
x_{12}(0) &= [2500, 0.13, 1.312865, 6.37\times10^{-5}]^T,\\
P_{11}(0) &= \mathrm{diag}\{25, 1\times10^{-6}, 9\times10^{-6}, 4.5\times10^{-8}\},\\
P_{12}(0) &= \mathrm{diag}\{16, 1\times10^{-6}, 9\times10^{-6}, 5.6\times10^{-8}\},\\
x_2(0) &= [100, 220]^T, Q_2 = 16.
\end{aligned}$$

Since all the existing OTHR based tracking methods just work in the case that the ionospheric heights are given, we compare the proposed IMSF (without knowing the ionospheric heights) with the well-known MPDA (with knowing the ionospheric heights). As shown in Figs. 3-4, our IMSF is almost as accurate as the MPDA, this is because though the prior information about the ionospheric heights is not known in our IMSF, its updating model is established which compensates the missing of information about the ionospheric heights. As shown in Figs. 5-6, the ionospheric heights can be estimated by our IMSF.

V. Conclusion

In this paper, we present the multi-rate joint estimation problem of target state and ionosphere state without the help of ionosondes. The state equations and observation equation have random coefficient matrices (RCM) due to the association uncertainty. The multi-rate state filter in the LMMSE sense is derived according to the orthogonality principle in the linear case and further extended to the non-linear case via the iterative optimization of joint state estimation and parameter identification (the linearized measurement matrix). A numerical example shows the effectiveness of the proposed filter.

Acknowledgments

This research is supported by the National Science Foundation Council of China under Grant 61135001, 61074179, 61374023, 61374159 and 61403309, ASTC through grant 2014-HT-XGD, the Fundamental Research Funds for the Central Universities of China through grant 3102014KYJD030, and the Innovation Foundation for Doctor dissertation of Northwestern Polytechnical University under grant CX201505.

Proof of Theorem. 1

According to the orthogonality principle, the LMMSE filter has the following expression:

$$\hat{\underline{x}}_k^e = \hat{\underline{x}}_k^p + \underline{K}_k\left(\underline{z}_k - \hat{\underline{z}}_{k|k-1}\right),$$

where $\hat{\underline{z}}_{k|k-1} = E\left\{\underline{z}_k|\underline{z}_j, j<k\right\}$. Noting $E\{\underline{v}_k\}=0$, and $\underline{v}_k$ is independent of $\underline{Z}^{k-1}$, we substitute the definition of $\hat{\underline{x}}_k^p$ into the definition of $\hat{\underline{z}}_{k|k-1}$ and hence we have

$$\begin{aligned}
\hat{\underline{z}}_{k|k-1} &= E\left\{\underline{C}_k\underline{x}_k + \underline{v}_k|\underline{Z}^{k-1}\right\}\\
&= \underline{C}_k E\left\{\underline{x}_k|\underline{Z}^{k-1}\right\} + E\left\{\underline{v}_k|\underline{Z}^{k-1}\right\}\\
&= \underline{C}_k\hat{\underline{x}}_k^p.
\end{aligned}$$

Expanding the above equation into its sub-block form, we have (22).

By noting that $E\{\underline{w}_k\}=0$ and $\underline{w}_{k-1}$ is independent of $\underline{Z}^{k-1}$, utilizing the definition $\hat{\underline{x}}_k^p = E\{\underline{x}_k|Z^k\}$ and (14), we have

$$\begin{aligned}
\hat{\underline{x}}_k^p &= E\left\{\underline{A}x_{k-1} + \underline{B}u_{k-1} + \Gamma\underline{w}_{k-1}\right\}\\
&= \underline{A}E\left\{\underline{x}_{k-1}|\underline{Z}^{k-1}\right\} + \underline{B}E\left\{\underline{u}_{k-1}|\underline{Z}^{k-1}\right\}\\
&\quad + E\left\{\underline{\Gamma w}_{k-1}|\underline{Z}^{k-1}\right\}\\
&= \underline{A}\hat{\underline{x}}_{k-1}^e + \underline{B}\underline{u}_{k-1}.
\end{aligned}$$

Based on this equation and the definition $\hat{\underline{x}}_k^p = E\{\underline{x}_k|Z^k\}$, we get (18) and (21).

According to the expression of $\hat{\underline{x}}_k^e$ and (18), we get (19) and (20).

According to the definition of $\underline{P}_k^p$ and $\underline{P}_k^e$, we have

$$\begin{aligned}
\underline{P}_k^p &= E\left\{\left(\underline{A}\tilde{\underline{x}}_{k-1}^e + \underline{\Gamma w}_{k-1}\right)(\cdot)^T\right\}\\
&= \underline{A}\underline{P}_{k-1}^e + \underline{\Gamma}\underline{Q}_{k-1}\underline{\Gamma}^T,\\
\underline{P}_k^e &= E\left\{\left(\underline{x}_k - \hat{\underline{x}}_k^p - \underline{K}_k\left(\underline{C}_k\tilde{\underline{x}}_k^p + \underline{v}_k\right)\right)(\cdot)^T\right\}\\
&= E\left\{\left(\left(I - \underline{K}_k\underline{C}_k\right)\tilde{\underline{x}}_k^p - \underline{K}_k\underline{v}_k\right)(\cdot)^T\right\}\\
&= \left(I - \underline{K}_k\underline{C}_k\right)\underline{P}_k^p\left(I - \underline{K}_k\underline{C}_k\right)^T + \underline{K}_k\underline{R}_k\underline{K}_k^T.
\end{aligned}$$

Based on the special structure of $\underline{K}_k$, $\underline{P}_k^p$ and $\underline{P}_k^e$ can be rewritten in block style as (23)-(24).

The LMMSE performance index is

$$\begin{aligned}
&\min_{\underline{K}_k} E\left\{\left(\underline{x}_k - \hat{\underline{x}}_k^e\right)^T(\cdot)\right\}\\
=& \min_{\underline{K}_k}\sum_{i=1}^{N+1} E\left\{\left(\underline{x}_k^{(i)} - \hat{\underline{x}}_k^{e(i)}\right)^T(\cdot)\right\}\\
&= \sum_{i=1}^{N+1}\min_{K_k^i}\left\{E\left\{\left(\underline{x}_k^{(i)} - \hat{\underline{x}}_k^{e(i)}\right)^T(\cdot)\right\}\right\}.
\end{aligned}$$

Thus, minimizing the trace of the augmented state estimate error covariance matrix is equivalent to minimizing the original state estimate error. In other words, the LMMSE estimate of the lifted system with causality constraint is equivalent to the LMMSE estimate of the original multi-rate system. The augmented LMMSE estimate leads to an optimal estimate for each state.

On account of the causality constraint of the gain matrix, $\bar{K}_k$ is a non-free matrix containing large quantities of zero blocks. To solve the gain matrix, denote the causality constraint matrix $M_i = [I_{im}, O_{im\times(N-i)m}]$. The filter gain K_k^i is derived in two cases.

Case 1: $i \le N-1$

$$\begin{aligned}
\hat{\underline{x}}_k^{e(i)} &= \hat{\underline{x}}_k^{p(i)} + \left[\underline{K}_k^{i,1}, \cdots, \underline{K}_k^{i,i}, 0, \cdots, 0\right]\left[\underline{z}_k - \underline{C}_k\hat{\underline{x}}_k^p\right]\\
&= \hat{\underline{x}}_k^{p(i)} + \underbrace{\left[\underline{K}_k^{i,1}, \cdots, \underline{K}_k^{i,i}\right]}_{K_k^i} M_i\left[\underline{z}_k - \underline{C}_k\hat{\underline{x}}_k^p\right]\\
&= \hat{\underline{x}}_k^{p(i)} + K_k^i\left[z_k^{(i)} - C_k^{(i)}\hat{\underline{x}}_k^p\right],
\end{aligned}$$

with

$$z_k^{(i)} = M_i \bar{z}_k = \mathrm{col}\{z_{kN}, \cdots, z_{kN+i+1}\},$$
$$C_k^{(i)} = M_i \bar{C}_k = \begin{bmatrix} I_i \otimes C_{1,k} & O_{i\times(N-i)} \otimes C_{1,k} & 1_i \otimes C_{2,k} \end{bmatrix}.$$

Up to this point, the problem has been transformed into calculating K_k^i, an unconstrained parameter matrix. Utilizing the orthogonal principle, it will be derived that

$$K_k^i = \underbrace{\mathrm{cov}\left(\underline{x}_k^{(i)} - \hat{\underline{x}}_k^{p(i)}, z_k^{(i)} - C_k^{(i)}\hat{\underline{x}}_k^p\right)}_{U_k^i} \times \underbrace{\mathrm{cov}^{-1}(z_k^{(i)} - C_k^{(i)}\hat{\underline{x}}_k^p, z_k^{(i)} - C_k^{(i)}\hat{\underline{x}}_k^p)}_{(V_k^i)^{-1}},$$

$$\begin{aligned} U_k^{(i)} &= E\left\{\hat{\underline{x}}_k^{p(i)}\left(C_k^{(i)}\hat{\underline{x}}_k^p + v_k^i\right)^T\right\} \\ &= E\left\{\hat{\underline{x}}_k^{p(i)}(\hat{\underline{x}}_k^p)^T\right\}\left(C_k^{(i)}\right)^T \\ &= \left[\underline{P}_k^{p(i,1)}\underline{P}_k^{p(i,2)}\cdots\underline{P}_k^{p(i,i)}\right]C_{1,k}^T \\ &\quad + 1_i^T \otimes \underline{P}_k^{p(i,N+1)} C_{2,k}^T, \end{aligned}$$

$$V_k^{(i)} = E\left\{\left(C_k^{(i)}\hat{\underline{x}}_k^p + v_k^i\right)(\cdot)^T\right\} = C_k^{(i)}\underline{P}_k^p\left(C_k^{(i)}\right)^T + \underline{R}_k^{(i)},$$

with

$$v_k^{(i)} = \mathrm{col}\{v_{kN}, \cdots, v_{kN+i-1}\},$$
$$\underline{R}_k^{(i)} = \mathrm{diag}\{R_{kN}, \cdots, R_{kN+i-1}\}.$$

Case 2: $i = N, N+1$
By the fact that K_k^i is not constrained , based on the orthogonal principle, we immediately have $K_k^{(i)} = U_k^i\left(V_k^{(i)}\right)^{-1}$, where $U_k^{(i)} = \left[\underline{P}_k^{p(i,1)}\cdots\underline{P}_k^{p(i,N)}\right]C_{1,k}^T + 1_N^T \otimes \underline{P}_k^{p(i,N+1)} C_{2,k}^T$, $V_k^i = \underline{C}_k\underline{P}_k^p\underline{C}_k^T + \underline{R}_k^{(i)}$, i.e., (25).

REFERENCES

[1] M. Headrick and J. Thomason, "Applications of high-frequency radar," *Radio Sci*, vol. 33, no. 4, pp. 1045-1054, 1998.

[2] D. Andrisani and C. Gau, "Estimation using a multirate filter," *IEEE Trans. on Autom. Control*, vol. 32, pp. 653-656, 1987.

[3] I. Dall and D. Kewley, "Track association in the presence of multi-mode propagation," *IEEE Conference Publication*, vol. 365, pp. 70-73, 1992.

[4] L. McNamara, "The ionosphere: communications, surveillance, and direction finding, " Malabar, FL: Kreiger, 1991.

[5] M. Lees, "An overview of signal processing for an over-the-horizon radar," *In Proc. of the ISSPA'87*, Brisbane, 1987, pp. 491-494.

[6] G. Pulford, A. Logothetis and R. Evans, "Integrated multipath track initiation for over-the-horizon radar: 3rd report to Telecom Australia," CSSIP report, vol. 95, no. 3, Adelaide, 1995.

[7] W. Torrez, and W. Yssel, "Over-the-horizon radar surveillance sensor fusion for enhanced coordinate registration," *IEEE Proc. on Information, Decision and Control*, 1999, pp. 227-230.

[8] B. Weijers and D. Choi, "OTHR-based coordinate registration experiment using an HF beacon," *Proc. Int. Conf. on Radar*, 1993, pp. 49-52.

[9] G. Pulford, R. Evans, "A multipath data association rracker for over-the-horizon radar," *IEEE Trans. Aerosp. Electron. Syst*, vol. 34, no. 4, pp. 1165-1183, 1998.

[10] G. Pulford, "Over-the-horizon radar multipath tracking with uncertain coordinate registration," *IEEE Trans. Aerosp. Electron. Syst*, vol. 40, no. 1, pp. 38-56, 2004.

[11] H. Liu, Y. Liang, Q. Pan, and Y. Cheng "Comments on a multipath data association tracker for over the-horizon radar," *IEEE Trans. Aerosp. Electron. Syst*, vol. 41, no. 3, pp. 1147-1150, 2005.

[12] S. Davey and D. Gray, "A comparison of track initiation methods with the PMHT," *Proc. Conf. Information, Decision and Control*, 2002, pp. 323-328.

[13] P. Willett, Y. Ruan and R. Streit, "The PMHT: problems and some solutions," *IEEE Trans. Aerosp. Electron. Syst*, vol. 38, no.3, pp. 738-754, 2002.

[14] G. Pulford and B. Scala, "Over-the-horizon radar tracking using the Viterbi algorithm," Third Report to High Frequency Radar Division, August 1995, pp. 27-95.

[15] H. Liu, Y. Liang, Q. Pan, and Y. Cheng, "A multipath viterbi data association algorithm for OTHR," CIE International Conference of Radar Proc, 2007.

[16] T. Sathyan, T. Chin, S. Arulampalam, and D. Suter, "A multiple hypothesis tracker for multitarget tracking with multiple simultaneous measurements," *IEEE J. Sel. Topics Signal Process*, vol. 7, no. 3, pp. 448-460, 2013.

[17] B. Habtemariam, R. Tharmarasa, T. Thayaparan, and M. Mallick, "A multiple-detection joint probabilistic data association filter," *IEEE J. Sel. Topics Signal Process*, vol. 7, no. 3, pp. 461-471, 2013.

[18] H. Lan, Y. Liang, Q. Pan, F. Yang, and C. Guan, "An EM algorithm for multipath state estimation in OTHR target tracking," *IEEE Trans. Signal Process*, vol. 62, no. 11, pp. 3814-3826, 2014.

[19] A. Orkun, "Forecasting of ionospheric critical frequency using neural networks," *Geophys. Res. Lett*, vol. 24, no. 12, pp. 1467-1470, 1997

[20] I. Stanislawska and G. Juchnikowski, "Generation of instantanneous maps of ionospheric characteristic," *Radio Sci*, vol. 36, no. 5, pp. 1073-1081, 2001.

[21] J. Bucknam, "Beacon-assisted vectoring of aircraft with OTH radar," Rome Lab. Technical Report, RL-TR-94-211, 1994.

[22] L. Jeffrey and H. Richard, "Maximum likelihood coordinate registration for over-the-horizon radar," *IEEE Trans. Signal Process*, vol. 45, no. 4, pp. 945-959, 1997.

[23] G. Frazer, "Forward-based receiver augmentation for OTHR," *IEEE Radar Conference*, 2007, pp. 373-378.

[24] X. Feng, Y. Liang, and L. Zhou, "Joint mode identification and localisation improvement of over-the-horizon radar with forward-based receivers," *IET Radar, Sonar and Navigation*, vol. 8, no.5, pp. 490-500, 2014.

[25] T. Fortmann, Y. Bar-Shalom and M. Scheffe, "Multi-target tracking using joint probabilistic data association," *In Proc. of the 19th IEEE Decision and Control including the Symposium on Adaptive Processes Conference*, 1980.

[26] T. Chen and B. Francis, "Optimal sampled-data control systems," New York: Springer-Verlag, 1995.

[27] B. Bell, and F. Cathey, "The iterated Kalman filter update as a Gauss-Newton Method," *IEEE Trans. Autom. Control*, vol. 38, no. 2, pp. 294–297, 1993.

[28] R. Bellaire, E. Kamen, and S. Zabin, "A new nonlinear iterated filter with applications to target tracking," *Proc. SPIE 2561, Signal and Data Processing of Small Targets*, 1995, pp. 240–251.

[29] R. Zhan, and J. Wan"Iterated unscented Kalman filter for passive target tracking," *IEEE Trans. Aerosp. Electron. Syst.*, vol. 43, no. 3, pp. 1155–1163, 2007.

[30] Y. Qin, Y. Liang, and Y. Yang, "Adaptive filter of non-linear systems with generalised unknown disturbances," *IET Radar, Sonar and Navigation*, vol. 8, no. 4, pp. 307-317, 2014.